UNIVERSITA' DEGLI STUDI DI MILANO BICOCCA

FACOLTA' DI SCIENZE MATEMATICHE FISICHE E NATURALI
DIPARTIMENTO DI FISICA "GIUSEPPE OCCHIALINI"
ACADEMIC YEAR 2022-2023

Essay for the Computational Physics Laboratory exam

Topological susceptibility in SU(3) Yang-Mills theory

Abstract

In this work the analysis of data obtained through Monte Carlo simulations of the SU(3) Yang-Mills theory is presented. A naive definition of the topological charge density evolved via Y-M gradient flow is implemented and the topological charge distribution of the theory is studied. By computing the second cumulant of the topological charge distribution the value of the topological susceptibility is extracted. Furthermore, it is shown numerically that the cumulants of the topological charge distribution defined at different flow times share the same universality class in the continuum limit. The numerical results obtained for the topological susceptibility in the pure Gauge theory allows a non perturbative implementation of Witten and Veneziano formula, which is used to compute the anomalous mass of the η' meson. The best results obtained in this work are $M_{\eta'} = 957.95(3.31)$ and $\chi = [179.23(2.03)\texttt{MeV}]^4$.

Professor: Leonardo Giusti
Candidate: Federico De Matteis

Contents

1 Preliminaries in the continuum

In the continuum, QCD is described by the SU(3)-defining Gauge symmetry of color. The action of QCD is described in the continuum by the sum of the gluonic and fermionic actions $S_F + S_G$, where:

$$\begin{aligned} S_G &= \frac{1}{2g_0}\int d^4x \mathrm{Tr}[F_{\mu\nu}F_{\mu\nu}], \\ S_F &= \int d^4x \left\{\bar{\Psi}\gamma_\mu D_\mu + m\right\}\Psi. \end{aligned} \tag{1.0.1}$$

In nature the $U(1)_A$ symmetry is broken by the quantization of the theory due to the non-invariance of the fermionic measure in the path integral (PI) under this chiral subgroup, giving rise to the chiral anomaly. The origin of the anomaly is of non-perturbative nature and lattice QCD represents the tool to investigate the anomalous s.b. mechanism and its consequences. In what follows, the non-perturbative treatment of the fermionic and the pure Gauge actions are addressed separately.

2 Lattice QCD

2.1 The pure Yang-Mills action

The discrete version of the pure gauge action for the SU(3) Yang-Mills theory is

$$S_G = \frac{\beta}{2}\sum_x \sum_{\mu,\nu}\left[1 - \frac{2}{N_c}\mathrm{Tr}\left\{U_{\mu\nu}(x) + U^\dagger_{\mu\nu}(x)\right\}\right], \tag{2.1.1}$$

where N_c is the number of colours considered, $\beta = \frac{2N_c}{g_0}$ and g_0 is the coupling constant. The fundamental degree of freedom of the theory is the parallel transport, defined as:

$$U_\mu(x) = e^{-i\mathtt{a}A_\mu}, \tag{2.1.2}$$

and it belongs to the gauge group itself. Here A_μ is the gauge field and $\mathtt{a}$ is the lattice spacing, while $U_{\mu\nu}(x)$ is the smallest closed path on the lattice obtained as a product of parallel transports (or links), namely the Wilson plaquette:

$$U_{\mu\nu} = U_\mu(x)U_\nu(x+\hat{\mu})U^\dagger_\mu(x+\hat{\mu})U^\dagger_\nu(x). \tag{2.1.3}$$

$U_{\mu\nu}$ is a gauge covariant object due to way the links behaves under a gauge transformation, and its trace $\mathrm{Tr}[U_{\mu\nu}(x)]$ is gauge invariant. Starting from Eq. (2.1.3) and using the Campbell-Hausdorff formula is possible to rewrite the Wilson plaquette as

$$U_{\mu\nu} = e^{-i\mathtt{a}^2[F_{\mu\nu}+\mathcal{O}(\mathtt{a}^2)]}, \tag{2.1.4}$$

and substituting Eq. (2.1.4) in Eq. (2.1.1) the gluonic action takes the form

$$S_G = \frac{1}{2g_0^2}\mathtt{a}^4\sum_x\sum_{\mu,\nu}\mathrm{Tr}\left[F_{\mu\nu}(x)F_{\mu\nu}(x)\right] + \mathcal{O}(\mathtt{a}), \tag{2.1.5}$$

which differs from the action of the continuum by discretization errors of order of the lattice spacing $\mathtt{a}$ which are themselves gauge invariant; this ensures gauge invariance for the action in Eq. (2.1.1). Here $F_{\mu\nu}$ is a particular discretization of the strength field tensor, which is also given in [1].

2.2 Fermion fields and the interacting theory

In order to include fermions in the theory without falling into the doubling problem[1] the Wilson fermionic action has to be considered:

$$S_F = a^4 \sum_x \bar{\Psi} \{D_W + m\} \Psi, \tag{2.2.1}$$

where D_W is the Wilson-Dirac operator which reads:

$$D_W = \frac{1}{2}\{\gamma_\mu(\nabla^* + \nabla_\mu) + \nabla^*_\mu \nabla_\mu\}. \tag{2.2.2}$$

The last term in round brackets in Eq. (2.2.2) commutes with γ_5, for this reason the fourth condition of the Nielsen-Ninomyia theorem is not satisfied. When turning on the interaction the links $U_\mu(x)$ also appear in the backward and forward derivatives in Eq. (2.2.2), and a new kernel of the action is needed[2]. Ginsparg and Wilson proposed a milder way of breaking the chiral symmetry on the lattice than introducing Wilson's fermions by writing a relation for the kernel of fermionic action:

$$\gamma_5 D + D\gamma_5 = \frac{\mathtt{a}}{1+s} D\gamma_5 D, \tag{2.2.3}$$

where $|s| < 1$. Eq. (2.2.3) translates into a relation for the quark propagator:

$$D^{-1}\gamma_5 + \gamma_5 D^{-1} = \mathtt{a}\gamma_5 \tag{2.2.4}$$

which anticommutes with γ_5 minus a contact term, which is present due to the locality of the matrix γ_5. The Ginsparg-Wilson relation is satisfied by the Neuberger's operator which reads

$$D = \frac{1+s}{\mathtt{a}}\{1 + \gamma_5 \frac{Q}{\sqrt{Q}}\}, \tag{2.2.5}$$

where Q is the Wilson operator with a negative mass term:

$$Q = \gamma_5(\mathtt{a}D_W - 1 - s). \tag{2.2.6}$$

[1]The naive discretization of the fermionic action with including the standard chiral symmetry on the lattice brings to the discretization of a theory with 8 r.h fermions and 8 l.h. fermions.

[2]Nielsen and Ninomyia stated that also is the interacting theory the kernel of the action must not anti-commute with γ_5, because the theory cannot be invariant under exact chiral symmetry, if not, in fact, the chiral symmetry breaking would not occur.

2.3 Luscher symmetry

The Neuberger's operator satisfies the modified chiral symmetry discovered by Luscher, who introduces a new definition for γ_5 on the lattice which tends to the standard definition in the continuum:

$$\hat{\gamma}_5 = (1 - \frac{\mathtt{a}}{1+s}\mathrm{D})\gamma_5, \tag{2.3.1}$$

and which depends on the gauge field (via the dependence on D). By means of this definition the Ginsparg-Wilson relation (2.2.3) can be written:

$$\gamma_5\mathrm{D} + \mathrm{D}\hat{\gamma}_5 = 0. \tag{2.3.2}$$

The fermionic action invariant under the Luscher symmetry is written as

$$\mathrm{S_F} = \mathtt{a}^4 \sum_x \bar{\Psi}(x)\,[\mathrm{D}\Psi]\,(\mathtt{x}). \tag{2.3.3}$$

The sum of the gluonic and fermionic actions in Eq. (2.1.1) and Eq. (2.2.3) is taken as the QCD action on the lattice and it is invariant under the Luscher symmetry as explained in the previous sub-sections.

2.4 The Chiral anomaly

When inserting the QCD action in the path integral in order to quantize the theory:

$$\mathcal{Z} = \int d\mathrm{U} d\Psi d\bar{\Psi} e^{-(\mathrm{S_F}+\mathrm{S_G})} \tag{2.4.1}$$

the fermionic measure $d\bar{\Psi}d\Psi$ is not invariant under the Luscher's symmetry, giving rise to the chiral anomaly. Indeed under this symmetry fermion fields transform as:

$$\Psi' = e^{i\epsilon^0_{\mathrm{A}}\hat{\gamma}_5}\Psi \qquad \Psi' = e^{i\epsilon^0_{\mathrm{A}}\gamma_5}\Psi, \tag{2.4.2}$$

where ϵ^0_{A} is the parameter linked to the axial $\mathtt{U}(1)_{\mathtt{R-L}}$ phase transformation acting on right and left quark fields with opposite phases. In fact by performing a change of variables using Grassmanian fields[3] and using the property $\mathrm{Tr}[\gamma_5] = 0$, the fermionic measure in the PI in Eq. (2.4.1) transforms as:

$$d\bar{\Psi}'d\Psi' = e^{-i\epsilon^0_{\mathrm{A}}\mathrm{Tr}[\hat{\gamma}_5]}d\bar{\Psi}d\Psi \tag{2.4.3}$$

where the trace is taken over color and Dirac indices and over space time indices. In addition, by exploiting the definition of $\hat{\gamma}_5$ in Eq. (2.3.1) the trace in Eq. (2.4.3) can be rewritten as

$$\mathrm{Tr}[\hat{\gamma}_5] = -\frac{\mathtt{a}}{1+s}\sum_x tr[\gamma_5\mathrm{D}(x,x)], \tag{2.4.4}$$

where the small trace is taken over color and Dirac indices only. The Ginsparg-Wilson definition of the topological charge density is introduced as

$$\mathtt{a}^4 q(x) = -\frac{\mathtt{a}}{2(1+s)} tr[\gamma_5\mathrm{D}(x,x)], \tag{2.4.5}$$

[3]The fermionic measure in the PI becomes $d\bar{\Psi}'d\Psi' = \frac{1}{det(e^{i\epsilon^{\mathrm{A}}_0\gamma_5})}\frac{1}{det(e^{i\epsilon^{\mathrm{A}}_0\hat{\gamma}_5})}d\bar{\Psi}d\Psi$.

and the discrete version of the integral of $q(x)$, namely the topological charge Q, can be written as

$$\mathrm{Q} = a^4 \sum_x q(x) = \frac{1}{2}\mathrm{Tr}[\hat{\gamma}_5]. \tag{2.4.6}$$

By studying the spectral properties of the Neuberger's operator it is possible to connect the number of its zero modes with positive and negative chirality (n^+, n^-) in a given gauge field configuration and the trace of $\hat{\gamma}_5$, leading to the expression for the topological charge:

$$\mathrm{Q} = (n^+ - n^-). \tag{2.4.7}$$

The topological charge Q is a gluonic quantity, despite it is obtained by tracing a fermionic matrix, and its value is constant under the variation of fermionic fields.

2.5 Topological charge and its cumulants

On the lattice it is necessary to obtain a definition of the topological charge whose cumulants have an unambiguous continuum limit not affected by short distance singularities [1]. Such a definition can be introduced by a naive discretization of Q that implements the Yang-Mills(Y-M) gradient flow. This evolves the gauge field A_μ as a function of the positive flow time $\mathtt{t}$, corresponding to obtain a smooth renormalized gauge field, by solving the Y-M gradient flow equation [1]. Starting from the Neuberger's definition of the topological charge in Eq. (2.4.6) evolved in the flow time, where $q(x)$ is the definition of topological charge density given in Eq. (2.4.6), we can define the cumulants of the topological charge distribution as

$$\mathrm{C}_n^{\mathtt{t}} = \frac{a^{8n-4}}{\mathrm{V}} \sum_{x_1 \ldots x_{2n-1}} \langle q^{\mathtt{t}}(x_1) \ldots q^{\mathtt{t}}(x_{2n-1}) q^{\mathtt{t}}(0) \rangle. \tag{2.5.1}$$

The topological susceptibility is obtained by choosing $n = 2$ in Eq. (2.5.1) and is given by

$$\chi^{\mathtt{t}} = \frac{\langle [\mathrm{Q}^{\mathtt{t}}]^2 \rangle}{\mathrm{V}}. \tag{2.5.2}$$

For the flow time $\mathtt{t} > 0$ the cumulants have a universal continuum limit, and moreover in [1] is shown that the continuum limit of the cumulants $\mathrm{C}_n^{\mathtt{t}}$ coincides with the one of $\mathrm{C}_n^{\mathtt{t}=0}$. On the lattice it is possible to implement a definition for the topological charge density[1], which shares with the Neuberger's definition given in Eq. (2.4.5) the same asymptotic behavior in the continuum limit. In [1] the naive discretization used for the topological charge density evolved at a positive flow time $\mathtt{t}$ is

$$q^{\mathtt{t}}(x) = \frac{1}{64\pi^2} \epsilon_{\mu\nu\rho\sigma} \mathrm{G}_{\mu\nu}(x) \mathrm{G}_{\rho\sigma}(x), \tag{2.5.3}$$

here $\mathrm{G}^{\mathtt{a}}_{\mu\nu}(x)$ is the strength field tensor taken as in [1]:

$$\mathrm{G}^{\mathtt{a}}_{\mu\nu}(x) = -\frac{1}{4\mathtt{a}^2} tr[(\mathrm{Q}_{\mu\nu}(x) - \mathrm{Q}_{\nu\mu}(x))\mathrm{T}^{\mathtt{a}}], \tag{2.5.4}$$

where $\mathrm{Q}_{\mu\nu}$ is taken as in [1] and depends on the gauge field evolved in the positive flow time (denoted with $\mathrm{V}_\mu(x)$).

2.6 The Witten and Veneziano relation

The topological susceptibility in the pure Yang-Mills theory turns out to be fundamental in solving the problem of the anomalous large mass of the η' meson in QCD. This problem was understood by Witten and Veneziano who proposed a relation that holds in the chiral limit, and in the limit of a large number of colors $N_f/N_c \to 0$:

$$\chi^{YM} = lim_{\frac{N_f}{N_c}\to 0} lim_{m\to 0} \frac{F_\pi^2(M_{\eta'}^2 + M_\eta^2 - 2M_K^2)}{2N_f}. \tag{2.6.1}$$

The leading contribution to the mass anomaly of the η' meson can be obtained by computing the χ in a pure Yang and Mills theory, using the Witten and Veneziano relation in Eq. (2.6.1) to tie the vacuum expectation value of the squared topological charge directly to the mass of the η' meson via the topological susceptibility. The aim of this work is to reproduce the results found in [1], in which the topological susceptibility of the pure Y-M theory is computed, and show that the Mass of the η' meson can be extracted from this results by exploiting the Witten and Veneziano relation.

3 Numerical setup

Numerical simulations implement the standard Wilson plaquette action in Eq. (2.1.1) on a four-dimensional lattice with volume V and lattice spacing a. In tab. 1 is summarized the numerical setup for simulations conducted on three different lattices B_1, B_2 and B_3[4], the volume is kept constant and the value of the lattice spacing a is changed between them. The corresponding coupling constants and the scale parameters t_0/a^2 are also given, where t_0 is the reference flow time scale. Is to be noted that in order to compare the numerical results obtained on the lattice B_2 with those obtained in [1] it is necessary to consider the differences between the volumes used. The spatial extent of lattice B_2 here is L/a = 16, while in [1] L/a = 14 is used.[5]

lattice	β	cnfg	L/a	t_0/a^2	L[fm]
B_1	5.96	5886	12	2.7984(9)	1.2
B_2	6.05	4905	16	3.7960(12)	1.2
B_3	6.13	5004	16	4.8855(15)	1.2

Table 1: Parameters of simulations; the number of configurations used refers to the statistics before the binning procedure (see sub-section 3.1).

[4]The names for the lattices used in the same used in [1]

[5]In order to equalize the topological susceptibility obtained from equation (2.5.2) with that obtained in [1] for the simulation on the lattice B_2, $< [Q^t]^2 >$ is multiplied by the ratio $\frac{14}{16}$ and V = L/a = 14 is used in the analysis.

3.1 Autocorrelation test

The autocorrelation of the topological charge Q has been computed for the three simulations carried out; it is defined as:

$$\Gamma(t_M) = \langle Q_j Q_{j+t_M} \rangle - \langle Q_j \rangle^2, \tag{3.1.1}$$

where t_M stands for the distance in the Markovian time. Data obtained from lattices B_1 and B_2 showed slight autocorrelation; it was chosen to eliminate every second topological charge in order to reduce the autocorrelation (the term "binning" is used to indicate this procedure)[6]. In fig. 1 the autocorrelation of $Q^{t=0}$ is shown for the lattice B_2. After the binning procedure

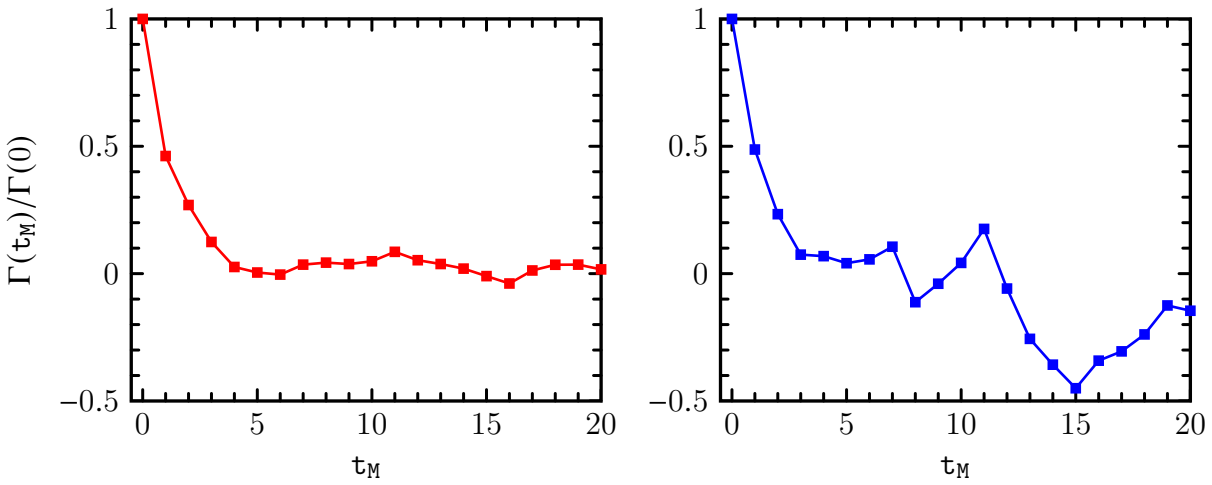

Figure 1: Lattice B_2: in the left plot the autocorrelation computed for the topological charge $Q^{t=t_0}$, in the right plot the autocorrelation is computed for $< Q^{t=t0} >$ after the binning procedure.

the fluctuations of $\frac{\Gamma(t)}{\Gamma(0)}$ increase because of the binning of the measurements of Q; also it seems that the binning procedure does not reduce the autocorrelation. Despite this, it is preferred to continue the analysis using binned data.

4 Physics results

4.1 Topological charge distribution

In fig. 2 are shown histograms of the topological charge measured at different flow times for the simulation on the lattice B_1. The plot for $t = 0$ shows a gaussian behavior, while increasing the flow time the topological charge tends to assume integer values and the non-gaussianity of the topological charge distribution becomes more visible. The second momentum of the topological charge distribution is computed for the different lattices, at different values of the flow time. The measurements were linearly interpolated at flow times correspondent to

[6] In order to maintain a similar number of measures on the three lattices also Q on lattice B_3 was binned; also it was noticed that proceeding without binning data for the lattice B_3 gains to less accurate results than those presented in section 5.

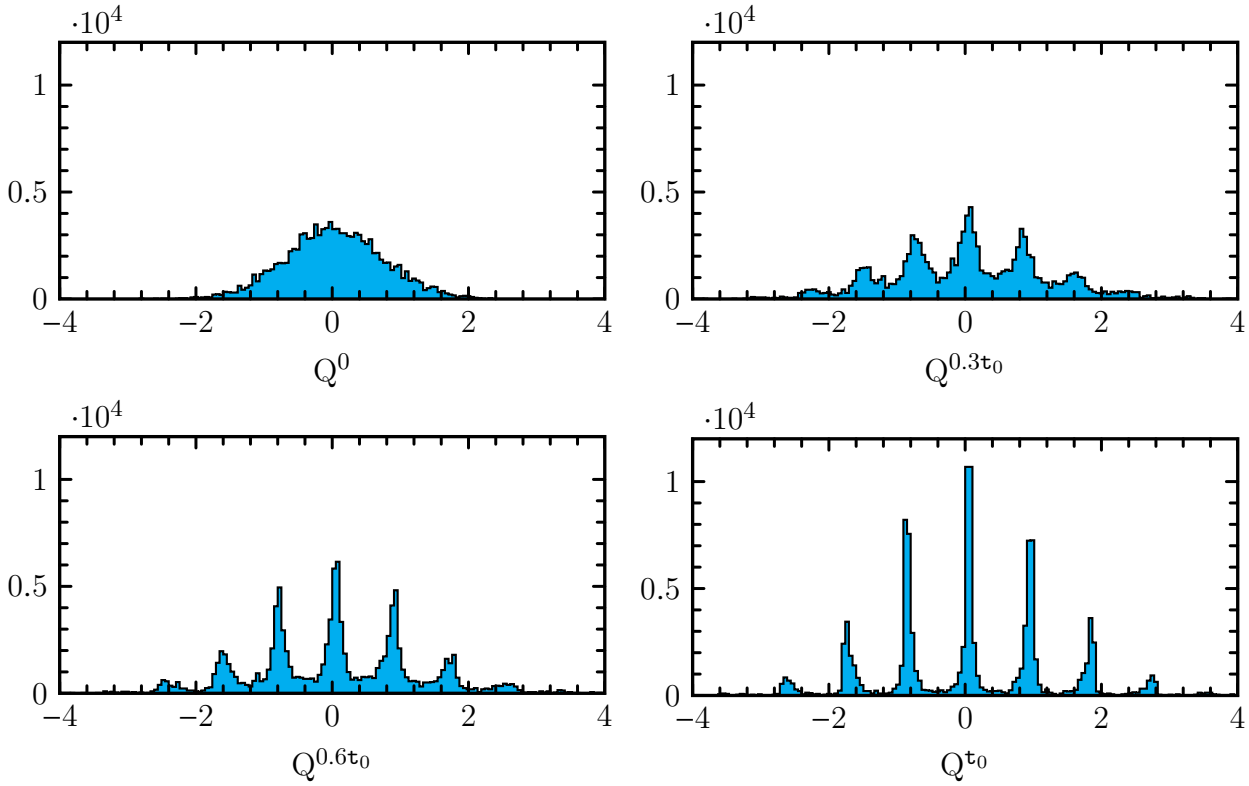

Figure 2: Topological charge measured for the different fractions of the reference flow time on the lattice $\mathtt{B}_1$.

different fractions of the reference scale $\mathtt{t}_0/\mathtt{a}^2$, by using the two nearest measures of $\langle[\mathrm{Q}^{\mathtt{t}}]^2\rangle$. In tab. 2 the numerical results are shown.

Lattice	$\langle \mathrm{Q}^{0.25\mathtt{t}_0}\rangle^2$	$\langle \mathrm{Q}^{0.25\mathtt{t}_0}\rangle^2$	$\langle \mathrm{Q}^{0.75\mathtt{t}_0}\rangle^2$	$\langle \mathrm{Q}^{\mathtt{t}_0}\rangle^2$	$\langle \mathrm{Q}^{1.25\mathtt{t}_0}\rangle^2$
$\mathtt{B}_1$	1.181(22)	1.455(30)	1.551(37)	1.601(46)	1.628(37)
$\mathtt{B}_2$	1.375(50)	1.558(63)	1.616(61)	1.652(60)	1.674(60)
$\mathtt{B}_3$	1.493(46)	1.637(47)	1.683(46)	1.711(45)	1.729(61)

Table 2: The second momentum of the topological charge distribution is computed after the binning procedure for different fractions of the reference flow time.

4.2 Topological susceptibility

The value of the topological susceptibility on the lattice is obtained by means of Eq. (2.5.2), by dividing the second momentum of the topological charge by the volume $\mathrm{V} = (\mathrm{L}/\mathtt{a})^4$, then the inverse of the squared reference scale parameter $(\mathtt{t}_0/\mathtt{a}^2)^2$ is multiplied on both left and right hand sides to obtain $\mathtt{t}_0^2\chi^{\mathtt{t}}$. The error $\sigma(\mathtt{t}_0^2\chi^{\mathtt{t}})$ is computed by propagating the error on the second cumulant of the topological charge $\langle[\mathrm{Q}^{\mathtt{t}}]^2\rangle$ and considering negligible the error on the reference scale $\mathtt{t}_0/\mathtt{a}^2$. This procedure is repeated for each flow time considered, for

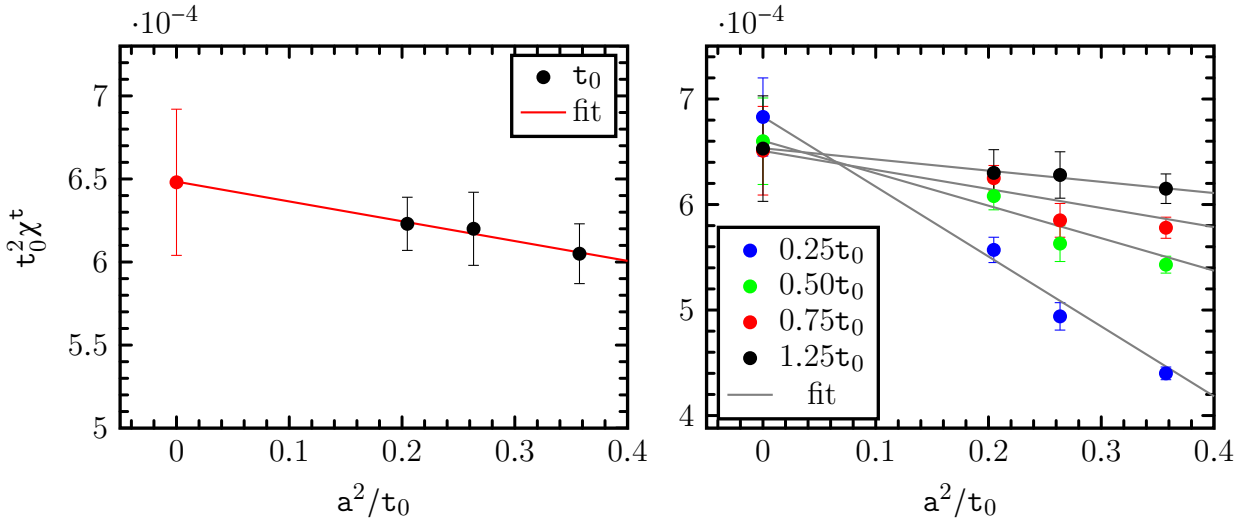

Figure 3: In the right plot the values of χt_0^2 extrapolated in the continuum limit for the three simulations for different flow times. On the left the continuum extrapolation of χt_0^2 at flow time $t = t_0$.

all the three simulations carried out. For each flow time a linear fit in a^2/t_0 is performed between the three values of $t_0^2\chi^t$ using the fit function:

$$f\left(\frac{a^2}{t_0}\right) = \alpha + \beta\frac{a^2}{t_0} \tag{4.2.1}$$

in order to estimate the fit parameters α and β and their errors. The continuum extrapolation of the quantity $t_0^2\chi^t$ is obtained by evaluating the fit function at $a^2/t_0 = 0$. The error $\sigma(\chi t_0^2)$ extrapolated from the fit (at $a^2/t_0 = 0$) reduces to the error on the parameter α. Tab. 2 resumes the continuum extrapolations of the observables computed. It is noted that the numerical values of $t_0^2\chi^t$ are compatible with the result:

$$t_0^2\chi = 6.67(7) \times 10^{-4} \tag{4.2.2}$$

presented in Eq. [5.2] in [1] within 0.5 standard deviations, for all the values of the flow time considered. It should be emphasized that the result held has an error of 1 order of magnitude greater than the result obtained in [1]. By dividing $t_0^2\chi$ by the square of the the reference flow time t_0^2 taken as in Eq. [5.3] in [1]:

$$t_0 = (0.176(4))^2, \tag{4.2.3}$$

we obtain χ in fm^4, which is translated into MeV^4. Again in tab. 2 we confront these results with the value obtained in Eq. [5.6] in [1]:

$$\chi = (180.5(5)MeV)^4. \tag{4.2.4}$$

4.3 Mass of the η' meson

The numerical values obtained for the topological susceptibility made it possible to compute the mass of the η' meson. By inverting the Witten-Veneziano relation in Eq. (2.6.1) the

mass of the meson is given by:

$$\mathcal{M}_{\eta'} = \left(\frac{6\chi}{F_\pi^2} - \mathcal{M}_\eta^2 + 2\mathcal{M}_K^2 \right)^{\frac{1}{2}}. \tag{4.3.1}$$

The error on $\mathcal{M}_{\eta'}$ is computed by propagating the errors on $\mathcal{M}_K$, $\mathcal{M}_\eta$ and on the Pion decay constant F_π. Although the first two can be considered null in errors propagation due to their order of magnitude with respect to the typical error found for the topological susceptibility. The values for the two masses and their corresponding errors are taken as $\mathcal{M}_\eta = 547.862(17)\texttt{MeV}$ and $\mathcal{M}_K = 493.677(16)\texttt{MeV}$ from [3]. From the same reference the value of the Pion decay constant F_π and its error can be obtained from the identity $f_\pi = \sqrt{2}F_\pi$, where $f_\pi = 130.2(8)\texttt{MeV}$ is used. In tab. 3 numerical results obtained for the η' mass are compared with the value found in [3].

$$\mathcal{M}_{\eta'} = 957.78(06)\texttt{MeV}. \tag{4.3.2}$$

The values found for $\mathcal{M}_{\eta'}$ correspondent to the fractions of the reference scale 0.75 and 1.25 respectively are presented as the best results in this analysis.

$\%(t_0/a^2)$	$t_0^2\chi^t$	$t(t_0^2\chi^t)$	$\left[\chi^t\texttt{MeV}\right]^4$	$t(\left[\chi^t\texttt{MeV}\right]^4)$	$\mathcal{M}_{\eta'}[\texttt{MeV}]$	$t(\mathcal{M}_{\eta'})$
0.25	$6.83(37) \times 10^{-4}$	0.43	181.24(2.06)	0.34	975.19(3.40)	5.11
0.5	$6.60(41) \times 10^{-4}$	0.16	179.71(2.04)	0.37	962.08(3.33)	1.29
0.75	$6.51(42) \times 10^{-4}$	0.38	179.05(2.03)	0.69	956.47(3.31)	0.40
1	$6.48(44) \times 10^{-4}$	0.42	178.88(2.03)	0.75	955.06(3.30)	0.82
1.25	$6.53(50) \times 10^{-4}$	0.05	179.23(2.03)	1.08	957.95(3.31)	0.27

Table 3: Physical observables results for different lattice simulations. with t the variable t-student in denoted.

4.4 Universality test

The value of the dimensionless ratio χ^t/χ^{t_0} is computed in order to confront the result with the one obtained in section 5.2 in [1]. Again the computation is carried out for all the flow times considered on the three lattices. As in sub-section 4.2 a linear fit between the values of χ^t/χ^{t_0} is performed using f in Eq. (4.2.1), then the continuum limit is extrapolated. Fig. 4 shows that the cumulants of the topological charge distribution converge at the same value as the lattice spacing runs towards zero, while at finite lattice spacing the discretization effects appear visible with different behaviors dependent on the flow time. The different continuum extrapolations approaches values all compatible with 1 inside the confidence level of 1 standard deviation. This result provides a universality test for the second cumulant of the topological charge distribution defined in Eq. (2.5.2), which is expected to be independent of the flow time in the continuum limit. The same is valid for the results shown in fig. 3 in sub-section 4.2 with higher confidence because to obtain an estimation of χ^t/χ^{t_0} it needs one more step in error propagation with respect to the estimation of χt_0^2. Finally we can compare the result obtained here for the topological susceptibility with the one obtained in [1]

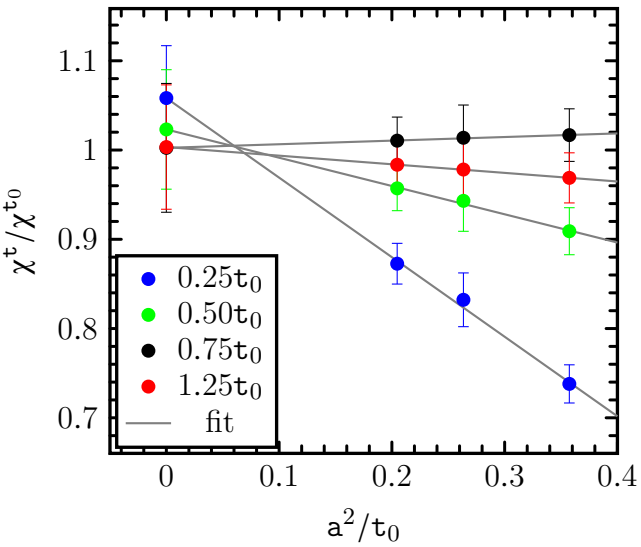

Figure 4: The dimensionless ratio computed for the different simulations and their extrapolation to the continuum limit for different fractions of the reference flow time scale.

$$r_0^4\chi = 0.0544(18). \tag{4.4.1}$$

The quantity $r_0^4\chi$ is obtained by dividing $t_0^2\chi$ by the ratio t_0/r_0^2, chosen as in table 3 in [1], corresponding to lattices B_1,B_2 and B_3 and it is compatible with the result in (4.4.1) within 1 standard deviations for all the flow times considered.

$\%(t_0/a^2)$	χ^t/χ^{t_0}	$t(\chi^t/\chi^{t_0})$	$r_0^4\chi$	$t(r_0^4\chi)$
0.25	1.058(59)	0.98	$5.56(12)\times10^{-2}$	0.58
0.5	1.023(67)	0.34	$5.37(12)\times10^{-2}$	0.28
0.75	1.003(69)	0.04	$5.30(12)\times10^{-2}$	0.65
1	1.000(71)	0.07	$5.28(11)\times10^{-2}$	0.74
1.25	1.002(72)	0.03	$5.32(12)\times10^{-2}$	0.55

Table 4: Physical observables results for different lattice simulations. The variable t-student is indicated with t and defined as usual: $t = (x-\tilde{x})/\sigma(x)$ where x is the value found from simulations and $\tilde{x}$ is the result against which the numerical results are compared.

5 Conclusions

The Yang-Mills gradient flow proves to be a useful tool to study the topological properties of the SU(3) Y-M theory and allows a naive definition of topological charge that is relatively cheap to be computed and whose cumulants share the same universality class in the continuum limit as the one given by Neuberger's fermions. It is noted that the results obtained for the topological susceptibility in section 4.2 show a bias towards values which are slight under the value obtained in [1]. Despite this, the results found for the topological susceptibility and for the mass of the η' meson can be considered satisfactory given the statistics used for this work.

6 Acknowledgments

The simulations were run on the Wilson HPC in the computational physics laboratory "Marco Comi" at University of Milano Bicocca, using the openQCD framework. Thanks are due to colleagues in the Computational Physics course with whom data from simulations were shared in order to increase statistics for data analysis.

References

[1] M. Cè, C. Consonni, G. P. Engel, L. Giusti, *Non-Gaussianities in the topological charge distribution of the SU(3) Yang–Mills theory*, 13 Sep 2015, arXiv:1506.06052v2 [hep-lat].

[2] L. Del Debbio, L. Giusti, C. Pica, *Topological susceptibility in SU(3) Gauge Theory*, 26 Jan 2005, 10.1103/PhysRevLett.94.032003.

[3] R.L. Workman et al. (Particle Data Group), Prog. Theor. Exp. Phys. 2022, 083C01 (2022) and 2023 update.